Batch-to-batch variation of polymeric photovoltaic materials

Lee, Harrison Ka Hin; Li, Zhao; Constantinou, Iordania; So, Franky; Tsang, Sai Wing; So, Shu Kong

Published in:
Advanced Energy Materials

DOI:
10.1002/aenm.201400768

Published: 01/11/2014

Document Version:
Peer reviewed version

Batch-to-Batch Variation of Polymeric Photovoltaic Materials: its Origin and Impacts on Charge Carrier Transport and Device Performances

Harrison Ka Hin Lee, Zhao Li, Iordania Constantinou, Franky So, Sai Wing Tsang*, Shu Kong So*

*Corresponding author

Harrison Ka Hin Lee, Prof. Shu Kong So

Department of Physics and Institute of Advanced Materials

Hong Kong Baptist University

Kowloon Tong, Hong Kong, China

E-mail: skso@hkbu.edu.hk

Dr. Zhao Li

Institute for Chemical Process and Environmental Technology

National Research Council of Canada

1200 Montreal Road, Ottawa, Canada ON K1A 0R6

E-mail: Zhao.Li@nrc-cnrc.gc.ca

Iordania Constantinou, and Prof. Franky So

Department of Materials Science and Engineering

University of Florida

Gainesville, Florida 32611-6400

E-mail: fso@mse.ufl.edu

Dr. Sai Wing Tsang

Department of Physics and Materials Science

City University of Hong Kong

Kowloon Tong, Hong Kong, China

E-mail: saitsang@cityu.edu.hk

Abstract

We report a detailed investigation on the impact of molecular weight distribution of a photoactive polymer, poly [N-9'-heptadecanyl-2,7-carbazole-alt-5,5-(4',7'-di-2-thienyl-2',1',3'-benzothiadiazole)] (PCDTBT), on photovoltaic devices performance and carrier transport properties. We found that different batches of as-received polymers have substantial differences in their molecular weight distribution. As revealed by gel permeation chromatography (GPC), two peaks can generally be observed. One of the peaks corresponds to a high molecular weight component and the other peak corresponds to a low molecular weight component. Photovoltaic devices fabricated with higher portion of low molecular weight component have reduced power conversion efficiencies (PCEs) from 5.7% to 2.5%. The corresponding charge carrier mobility at the short-circuit region has also been significantly reduced from 2.7 x 10^{-5} to 1.6 x 10^{-8} $cm^2V^{-1}s^{-1}$. The carrier transport properties of the polymers at various temperatures were further analyzed by the Gaussian disorder model (GDM). All polymers have similar energetic disorders. However, they appear to have significant differences in carrier hopping distances. This result brings insight into the origin of molecular weight effect on carrier transport in polymeric semiconducting materials.

1 Introduction

Solution processed bulk heterojunction (BHJ) organic photovoltaic (OPV) cells have attracted lots of attention due to the potential for making low-cost and high-efficiency devices. Over 9% power conversion efficiency (PCE) has been achieved on single junction cells.[1] During the last few years, a number of high efficiency, low-bandgap polymers have also reported with PCEs over 7%.[1-5] Such progress is contributed both by the development of more efficient materials and the optimization of device structure. To date, some of the high efficiency polymers are available commercially in small quantities for laboratory scale research and development. Quite often, these polymers are dispatched to the end users with incomplete specifications on its physical properties. As a result, batch-to-batch variations occur, and may lead to large fluctuations in device performances. Clearly, the batch-to-batch variation is a key obstacle for the commercialization of the technology in the future. The variation in performance is thought to be related to either trace metal content or molecular weight of the polymers.[6-9] Particularly, a strong dependence of molecular weight on the photovoltaic device performance has been demonstrated.[6-9] In general, devices fabricated with lower molecular weight polymers have lower carrier mobilities.[7,10-12] This increases the chance for carrier recombination and therefore reduces the photovoltaic performance. Unlocking the

origin of the reduced mobility is of the utmost importance for optimizing the device performance and understanding the carrier transport mechanism.

The batch-to-batch variation can arise from molecular weight variations for a given polymer. Different molecular weights may affect molecular packing. For example, poly(3-hexylthiophene) (P3HT) were shown to be beneficial to intermolecular ordering (π-stacking) of the polymers and lead to a higher carrier mobility in a thin film transistor (TFT) structure.[11] Similar results were also reported on two recently developed low bandgap polymers.[9,12,13] It was shown that PV devices fabricated with lower molecular weight polymers had significantly lower fill-factor (FF) and short-circuit current density (J_{SC}). It is worth to note that the carrier mobility obtained by TFT structure can only give a brief idea of the overall molecular weight effect. Due to the differences in device geometry and more importantly the relevant electric-field regimes where the carriers transport in TFT and OPV cell, the qualitative effect of different molecular weights on the physical parameters of carrier transport is still not clear. Nevertheless, previous studies on molecular weight effect mainly focused on polymers with strong π–π stacking which have clear X-ray diffraction patterns. However, similar molecular weight dependence has also been observed on an amorphous polymer, poly [N-9'-heptadecanyl -2,7

-carbazole-alt-5,5- (4',7'-di- 2-thienyl-2',1',3'- benzothiadiazole)] (PCDTBT).[8] Therefore, the crystallinity of the polymer might not be the only factor in controlling the carrier transport. The low molecular weight polymers would possibly either distort the energy of transporting sites or topological pathways for efficient carrier transport. This information is particularly important in order to understand the origin of the material and device inconsistencies.

Here we report a detailed investigation on the effect of batch-to-batch variation of molecular weight on PCDTBT photovoltaic devices and the corresponding carrier transport properties. Five different batches of PCDTBT were purchased and used as-received without further purification. The molecular weights of different batches were determined by gel permeation chromatography (GPC). The photovoltaic cells were fabricated using a blend of PCDTBT: (6,6)-phenyl C_{71}-butyric acid methyl ester ($PC_{71}BM$) (1:4 weight ratio) as the active layer. The general device structure is Indium-tin oxide(ITO)/MoO_3(15 nm)/PCDTBT:$PC_{71}BM$/LiF(1 nm)/Al. To see if molecular weight alters the intrinsic carrier transport properties in pristine polymer, we fabricated single carrier (hole-only) devices with PCDTBT from different batches. The current-voltage (J-V) characteristics of the hole-only devices at different temperatures were analyzed with the Gaussian disorder model (GDM) to extract the

carrier transport parameters.[14] The carrier transport results were used to compare the energetics of the transport sites and topological studies of the polymer thin films.

2 Results and discussion

2.1 Molecular Weight Distribution

GPC was performed to identify the variation of molecular weight on the five different batches of as-received PCDTBT. They were labeled in alphabetical order from A to E. Samples A-D were obtained from 1-Material while sample E was obtained from Luminescence Technology.[†] The results are shown in Figure 1. All PCDTBT samples have two peaks in the GPC analysis, which correspond to a high and a low molecular weight components. The high molecular weight component has a number average molecular weight (M_{n}) in the range of 70-110 kDa for different batches.(Table 1) Recently, Beaupré et al summarized the effect of molecular weight of PCDTBT on PV device performances.[8] They showed that a PCE larger than 5% can be obtained with polymers having M_{n} larger than 25 kDa. Therefore, the high molecular weight component of different batches should be within the desirable range for efficient PV devices. However, the major difference among different batches is the amount of the low molecular weight component with increasing quantity (peak intensity) from batch A to E. The low molecular weight component corresponds to M_{n} in a range of 2-10 kDa. The GPC results are summarized in Table 1. Depending on the amount of the low molecular weight component, the overall

[†] The selection of samples was based on what were available from the vendors at the time of this research. Our results here should not be interpreted as a systematical evaluation of polymers available from the venders.

average of M_{n}, $\overline{M_{\mathrm{n}}}$, varies from 27 kDa to 5 kDa. Figure 2 shows $\overline{M_{\mathrm{n}}}$ and the peak ratio of the high-to-low weight peaks of different batches of PCDTBT. It is well known that such combination of high and low molecular weight components is typical during polymerization. For instance, for PCDTBT, the polymers can be synthesized by condensation polymerization and the polydispersity depends on both the monomer ratio and the reaction conditions.[15] Particularly in high concentration, cyclization may take place and results in low molecular weight part. Consequently, without further extraction, the as-received polymers might have an uncertainty of such molecular weight distribution. Although the high M_{n} component is desirable for efficient PV device, the additional low M_{n} component would strongly affect the device performance.

2.2 OPV cells Performance

Figure 3 shows the J-V characteristics of the PV devices using different batches of PCDTBT under AM1.5G illumination. The highest PCE of 5.7% has been achieved with batch A, which has the least amount of low molecular weight component. The PCE is reduced with increasing amount of the low molecular weight component, and a PCE of only 2.5% can be obtained for batch E. The PV devices performance is summarized in Table 2. The correlation between the device performance and $\overline{M_{\mathrm{n}}}$ is

summarized in Figure 4. For samples A to D, the reduced PCE is mainly attributed to the lower J_{SC} and FF of the devices. The J_{SC} and FF were reduced from 10.7 mA/cm^2 to 9.1 mA/cm^2 and 58.5% to 47.8% respectively. We also note that there is an abrupt drop in device performance for sample E despite its molecular weight is similar to D. Sample E has a much reduced open-circuit voltage (V_{OC}) of 0.77 V compared to samples A-D. As companies might have different synthetic routes for a given polymer, a strict and quantitative comparison between sample E and the other four samples may not be reasonable. However, we still incorporate sample E in our discussion because it supports the notion that higher fraction of low molecular weight in PCDTBT suppresses the PV device performance.

We sought to investigate the cause of the reduced J_{SC} and FF from the perspectives of optical properties and molecular packing in different batches. As shown in Figure 5, the measured optical absorption spectra of the PCDTBT films are comparable among different batches. This result is different from previously reported polymers which have strong $\pi-\pi$ stacking.[9,11] In those cases, the thin films casted with high molecular weight polymers had higher optical absorption coefficients and had the cut-off absorptions towards longer wavelengths. On the other hand, thin films of PCDTBT are amorphous as prepared by spin coating. The differences in

optical absorption spectra and cut-offs are negligible from different batches. The amorphous nature is also confirmed by grazing incident X-ray diffraction (GIXRD) measurements as shown in Figure 6. There is absence of any notable diffraction peak in different batches of samples. Moreover, all PV devices have the same device structure and similar active layer thicknesses (70 nm). The amount of photon absorption and internal electric field should be comparable. Therefore, the lower J_{SC} and FF do not arise from weaker optical absorptions, but mainly originate from the reduced carrier mobilities from samples A to E.

2.3 Transport Study

In order to correlate the J_{SC} and FF of the photovoltaic devices with the carrier transport properties, we fabricated hole-only devices for current-voltage (J-V) measurement. The device structure is ITO/MoO_3/PCDTBT/Au for samples A to E. Carrier mobilities were extracted using the space-charge-limited current (SCLC) equation,[16-18]

$$J_{\mathrm{SCL}}d = \frac{9}{8}\varepsilon_0\varepsilon_{\mathrm{r}}\mu_0\exp\left(0.89\beta\sqrt{F}\right)F^2 \quad (1)$$

where J_{SCL} is the space-charged-limited current density, d is the thickness of polymer thin film, ε_0 is the permittivity of vacuum, ε_{r} is the relative permittivity of the polymer, μ_0 is the zero-field mobility, β is the field-dependent coefficient, and

F is the average electrical field. Figure 7a shows the room temperature data. (The fitted values of β are shown in Table S1 in supporting information) The current densities of the hole-only devices decrease from batch A to E. Batch A has a current four orders of magnitude larger than that of batch E. Moreover, the measured JV characteristics of devices are in good agreement with Eq (1). So, hole moiblities ($\mu_{\mathrm{Jsc}} = \mu_0 \exp(0.89\beta\sqrt{F})$) can be readily extracted where μ_{Jsc} is the carrier mobility corresponding to the short-circuit condition and *F* is the electric field at short-circuit condition. (Table 3, column 3) Temperature dependence J-V measurements were carried out to extract detailed carrier transport parameters. We employed the Gaussian disorder model (GDM) for analysis.[14] The model describes carrier hopping in energetically Gaussian distributed discrete transporting sites. The low field mobility can be described by:

$$\mu_0 = \mu_\infty \exp\left[-\left(\frac{2\sigma}{3kT}\right)^2\right] \quad (2)$$

where μ_∞ is the high-temperature limit mobility, σ is the energetic disorder parameter, k is the Boltzmann constant, and T is the absolute temperature. According to Eq. (2), the energetic disorder σ plays a key role in determining the carrier mobility. In fact, for a photoactive polymer, σ controls not only the mobility, but also the carrier recombination rate.[19] Several theoretical models have been proposed to correlate the fill-factor and open-circuit voltage with σ.[20,21]

Therefore, it is anticipated that the energetic disorder for different batches of polymers might be significantly different. In order to obtain σ, we measured μ_0 for each batch of PCDTBT at different temperatures. From a plot of μ_0 vs $1/T^2$, the slope can be used to extract σ.[22,23] Figure 7b shows a summary of these plots. Interestingly, the slopes from different batches are very similar, indicating that they have a similar value of σ. The carrier transport parameters are summarized in Table 3. In different batches, σ has almost the same values of 115±3 meV. In fact, instead of σ, the difference in carrier mobility in different batches is due to the difference in μ_∞, i.e. from μ_∞ = 2.0 x 10^{-2} $cm^2V^{-1}s^{-1}$ for batch A to μ_∞ = 1.2 x 10^{-5} $cm^2V^{-1}s^{-1}$ for batch E.

Figure 8 depicts how device performance is correlated with μ_∞. Following the concept of GDM, μ_∞ is proportional to the hopping distance, a, across the neighboring transporting sites. The high-temperature limit mobility can be described by:[24]

$$\mu_\infty \propto \exp(-2\gamma a) \quad (3)$$

where γ is the inverse localization radius. As γ is primarily determined by the molecular structure, it is reasonable to assume that it is a constant. Therefore, Eq.(3) suggests that the variation in carrier mobility in different batches is due to the

variation of hopping distances, a. In the case of a polymer with strong π–π stacking, such as P3HT, higher molecular weight is beneficial to promote intermolecular ordering, and therefore the hopping distance is smaller in higher crystalline thin film. On the other hand, thin film of PCDTBT is naturally amorphous that without notable XRD pattern (Figure 6), it is not clear on how the additional small molecular weight component can increase the overall hopping distance in PCDTBT. However, compared to P3HT, polymer chain of PCDTBT are non-planar.[25]. Such a non-planar polymer is unlikely to form closely packed domains, and the rate determining step for carrier transport is the probability of finding the lowest energy adjacent hopping sites. Although the intramolecular charge transfer is efficient along the polymer chain, the small molecular weight component in such non-planar and amorphous structure would hinder the intermolecular charge transfer as illustrated in Figure 9. Once a charge is transferred to a small molecular weight polymer chain, the probability of finding the nearest neighboring site to another chain is smaller than that of a long chain polymer. This results in increasing the overall hopping distances, and therefore reduced the carrier mobility.

Below, we want to further discuss other factors that may contribute to the batch-to-batch variations in PV performance. First, it is known that trace metal

content in polymer can be detrimental to device performances.[26] The amounts of trace metal concentrations in the PCDTBT, as revealed by both vendors, are in the order of 0.01-0.001 %.[27] This amount of trace metal should not contribute to our device performance as it was shown that at least 0.1 % of trace metal (e.g. Pd) is needed to induce any detrimental effect to OPV devices.[26]

Second, impurities other than trace metals might be present in our samples and lead to increased trap-assisted charge recombination. To address this issue, we measured the variations of V_{OC} on our BHJ samples with different incident light intensities.[28,29] Figure S2 in the supporting information shows the results for sample A, D, and E. If trap-assisted charge recombination is operative, we should see steeper slopes in Figure S2 from samples A to E. However, all three samples have a similar slope of kT/e suggesting increase in trap concentration is not the origin of reduced PCE from sample A to E.

Third, reduced mobilities may arise from contact-limited-charge injection.[30] To check if the measured mobilities in different samples are not limited by contact, we performed dark-injection space-charge-limited current (DI-SCLC) measurements on sample A to D.[16] Figure S3 in the supporting information shows the time-transients

of DI-SCLC. All data exhibited the classic features of DI-SCLC, with a current transient peak that signifies the transit time of the injected holes. The presence of such a transient peak indicates Ohmic contact for our samples.[22,31]

3 Conclusion

We have investigated in details the batch-to-batch variation of photovoltaic device performance and carrier transport properties using an amorphous polymer PCDTBT. We found that the additional small molecular weight component of the polymer significantly reduced both the device efficiency and carrier mobility. The reduction of mobility is not related to the increase of energetic disorder, instead the cause of the reduced carrier mobility is due to the larger hopping distances arising from the additional small molecular weight component. The results bring insight into the correlation between the topology of polymer chains and the carrier transport properties. This work not only provides a detail analysis of the effect of batch-to-batch variation of photoactive materials on device performance, but also provides a physical origin of the difference in carrier mobility and hence the resulting PV device performance.

4 Experimental Section

Materials: PCDTBT were purchased from 1-Material and Luminescence Technology. $PC_{71}BM$ was purchased from Nano-C. Anhydrous 1,2-dichlorobenzene (DCB) was obtained from Sigma Aldrich. These materials were used as received.

GPC: GPC (Waters Breeze HPLC system with 1525 Binary HPLC Pump and 2414 Differential Refractometer) was used for measuring the molecular weight and polydispersity index. Chlorobenzene was used as eluent and commercial polystyrenes were used as standard.

OPV cell Fabrication and Characterization: ITO patterned glass substrate was first cleaned with detergent and then sequentially cleaned in ultrasonic bath with deionized water, acetone, and isopropyl alcohol followed by UV-Ozone treatment. MoO_3 (99.998%, Strem Chemical) was thermally evaporated on ITO under high vacuum. The MoO_3 coated substrate was then transferred into a nitrogen filled glovebox (oxygen and moisture less than 1 ppm). PCDTBT and $PC_{71}BM$ were dissolved in DCB with the ratio of 1:4. The concentration of PCDTBT was 8 mg/ml. The solution was stirred at 90 ^{o}C for at least 16 hours and then filtered with a 0.45 μm syringe filter right before spin-coating. The solution was spin-coated onto the MoO_3 coated

ITO glass substrate resulting in ~70 nm thick blend layer. The film was dried naturally for 30 mins. Finally, 1 nm of lithium fluoride (LiF) and 130 nm of aluminum (Al) were thermally evaporated on the blend layer under high vacuum. The resulting device area was 0.108 cm^2. The sample for OPV cell had a structure of ITO/MoO_3/ PCDTBT:$PC_{71}BM$/LiF/Al. OPV cell measurement was carried out in air after evaporation using an AM 1.5G solar simulator with an intensity of 100 mW/cm^2. Keithley 2400 sourcemeter was used for the current-voltage measurement under light illumination.

Transport measurement: Hole-only device was fabricated for the SCLC measurement with the structure of ITO/MoO_3(20nm)/PCDTBT(~300nm)/Au. The fabrication procedure was similar to the OPV cell. 100 nm of gold (Au) was thermally evaporated on PCDTBT served as a high work function electrode to prevent electron injection. The resulting device area was 0.035 cm^2. Data were taken in an Oxford cryostat with pressure of less than 20 mTorr. The temperatures of the sample were regulated between 244 and 314 K.

Absorption: PCDTBT A to E solutions of were spin-coated onto quartzes. A PerkinElmer Lambda 750 UV/Vis Spectrometer was used for the measurement.

GIXRD: GIXRD measurements were performed by the Bruker D8 Advance X-ray Diffractrometer. The incident angle of X-ray was fixed at 0.3°, while the detector scanned from 3° to 30°.

Acknowledgements

Shu Kong So & Harrison Ka Hin Lee acknowledge supports from the Research Grant Council under grants #211412E and the Research Grants Council of the Hong Kong Special Administrative Region, China (Project No. [T23-713/11]). The GIXRD used in this work was supported by the Institute of Advanced Materials with funding from the Special Equipment Grant SEG-HKBU06. Sai Wing Tsang acknowledges the funding support from CityU start-up grant #7200372.

References

[1] Z. He, C. Zhong, S. Su, M. Xu, H. Wu, Y. Cao, *Nat. Photonics* **2012** ,*6* , 591.

[2] T. Y. Chu, S. Alem, S. W. Tsang, S. C. Tse, S. Wakim, J. Lu, G. Dennler, D. Waller, R. Gaudiana, Y. Tao, *Appl. Phys. Lett.* **2011** ,*98* , 253301.

[3] Y. Liang, L. Yu, *Acc. Chem. Res.* **2010**, *43*, 1227.

[4] C. E. Small, S. Chen, J. Subbiah, C. M. Amb, S. W. Tsang, T. H. Lai, J. R. Reynolds, F. So, *Nat. Photonics* **2012**, *6*, 115.

[5] T. Y. Chu, J. Lu, S. Beaupré, Y. Zhang, J. R. Pouliot, S. Wakim, J. Zhou, M. Leclerc, Z. Li, J. Ding, Y. Tao, *J. Am. Chem. Soc.* **2011**, *133*, 4250.

[6] R. C. Hiorns, R. Bettignies, J. Leroy, S. Bailly, M. Firon, C. Sentein, A. Khoukh, H. Preud'homme, C. Dagron-Lartigau, *Adv. Funct. Mater.* **2006**, *16*, 2263.

[7] C. Liu, K. Wang, X. Hu, Y. Yang, C. H. Hsu, W. Zhang, S. Xiao, X. Gong, Y. Cao, *Appl. Mater. Interfaces* **2013**, *5*, 12163.

[8] S. Beaupré, M. Leclerc, *J. Mater. Chem. A*, **2013**, *1*, 11097.

[9] T. Y. Chu, J. Lu, S. Beaupré, Y. Zhang , J. R. Pouliot, J. Zhou, A. Najari, M. Leclerc, Y. Tao, *Adv. Funct. Mater.* **2012**, *22*, 2345.

[10] A. M. Ballantyne, L. Chen, J. Dane, T. Hammant, F. M. Braun, M. Heeney, W. Duffy, I. McCulloch, D. D. C. Bradley, J. Nelson, *Adv. Funct. Mater.* **2008**, *18*, 2373.

[11] P. Schilinsky, U. Asawapirom, U. Scherf, M. Biele, C. J. Brabec, *Chem. Mater.* **2005**, *17*, 2175.

[12] S. Cho, J. H. Seo, S. H. Park, S. Beaupré, M. Leclerc, A. J. Heeger, *Adv. Mater.* **2010**, *22*, 1253.

[13] C. Müller, E. Wang, L. M. Andersson, K. Tvingstedt, Y. Zhou, M. R. Andersson, O. Inganäs, *Adv. Funct. Mater.* **2010**, *20*, 2124.

[14] H. Bässler, *Phys. Stat. Sol. B* **1993**, *175*, 15.

[15] N. Blouin, A. Michaud, M. Leclerc, *Adv. Mater.* **2007**, *19*, 2295.

[16] M. A. Lampert, P. Mark, *Current injection in solids*, Academic, New York **1970**.

[17] P. N. Murgatroyd, *J. Phys. D* **1970**, *3*, 151.

[18] S. C. Tse, S. W. Tsang, S. K. So, *J. Appl. Phys.* **2006**, *100*, 063708.

[19] S. Chen, C. E. Small, C. M. Amb, J. Subbiah, T. H. Lai, S. W. Tsang, J. R. Manders, J. R. Reynolds, F. So, *Adv. Energy Mater.* **2012**, *2*, 1333.

[20] J. C. Blakesley, D. Neher, *Phys. Rev. B* **2011**, *84*, 075210.

[21] G. Garcia-Belmonte, J. Bisquert Appl. Phys. Lett. **2010**, *96*, 113301

[22] K. K. H. Chan, S. W. Tsang, H. K. H. Lee, F. So, S. K. So, *Org. Electron.* **2012**, *13*, 850.

[23] K. K. H. Chan, S. W. Tsang, H. K. H. Lee, F. So, S. K. So, *J. Polym. Sci., Part B: Polym. Phys* **2013**, *51*, 649.

[24] A. Miller, E. Abrahams, *Phys. Rev.* **1960**, *120*, 745.

[25] J. Niklas, K. L. Mardis, B. P. Banks, G. M. Grooms, A. Sperlich, V. Dyakonov, S. Beaupré, M. Leclerc, T. Xu, L. Yu, O. G. Poluektov, *Phys. Chem. Chem. Phys.* **2013**, *15*, 9562.

[26] M. P. Nikiforov, B. Lai, W. Chen, S. Chen, R. D. Schaller, J. Strzalka, J. Maser, S. B. Darling, Energy Environ. Sci. **2013**, *6*, 1513.

[27] Information provided by 1-Material and Luminescence Technology, April 2014

[28] S. R. Cowan, A. Roy, A. J. Heeger, *Phys. Rev. B* **2010**, *82*, 245207.

[29] S. R. Cowan, W. L. Leong, N. Banerji, G. Dennler, A. J. Heeger, Adv. Funct. Mater. **2011**, *21*, 3083.

[30] Y. Shen, M. W. Klein, D. B. Jacobs, J. C. Scott, G. G. Malliaras, *Phys. Rev. Lett.* **2001**, *86*, 3867.

[31] D. Poplavskyy, J. Nelson, D. D. C. Bradley, Appl. Phys. Lett. **2003**, *83*, 707.

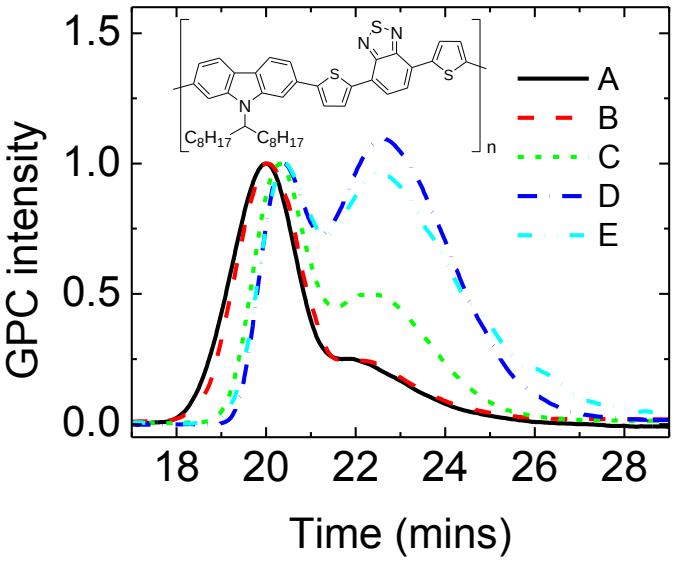

Figure 1. GPC results of five different batches (labeled A to E) of PCDTBT showing bimodal distributions of the molecular weight. A shorter time indicates higher molecular weight. The data were normalized to the high molecular weight peak. The inset shows the chemical structure of PCDTBT.

	Number average molecular weight, M_n (kDa)		
	High weight peak [*PDI*]	**Low weight peak [*PDI*]**	**Overall average, $\overline{M_n}$**
A	110.0 [2.2]	2.8 [1.2]	27.3
B	98.8 [2.0]	2.6 [1.3]	23.6
C	75.4 [1.4]	8.2 [1.1]	11.6
D	74.6 [1.2]	6.4 [1.3]	6.0
E	70.6 [1.3]	6.8 [1.2]	5.0

Table 1. GPC analysis of PCDTBT for sample A to E showing the number average molecular weight ($\boldsymbol{M_n}$) of the high and low molecular weight peaks. The overall average of the entire distribution ($\overline{M_n}$) is shown in the last column. Numbers within square parenthesis are the polydispersity indices (*PDI*) of the individual peaks.

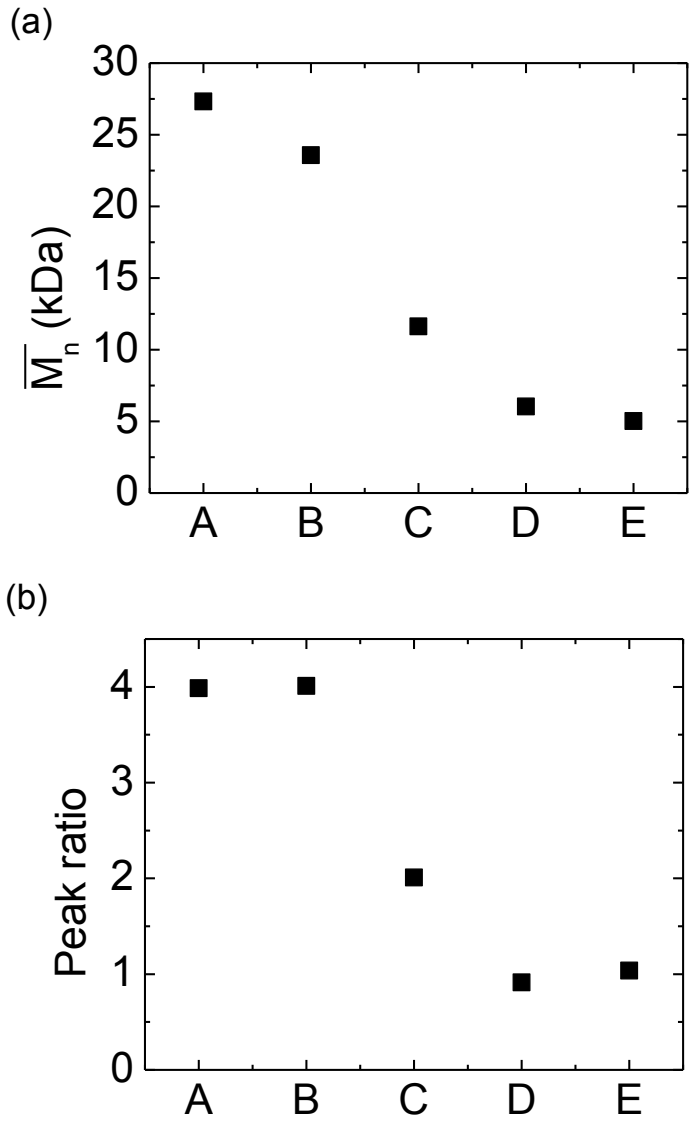

Figure 2. a, Overall average molecular weight, $\overline{M_{\mathrm{n}}}$. b, Peak height ratio (high-to-low molecular weight) of PCDTBT samples A to E.

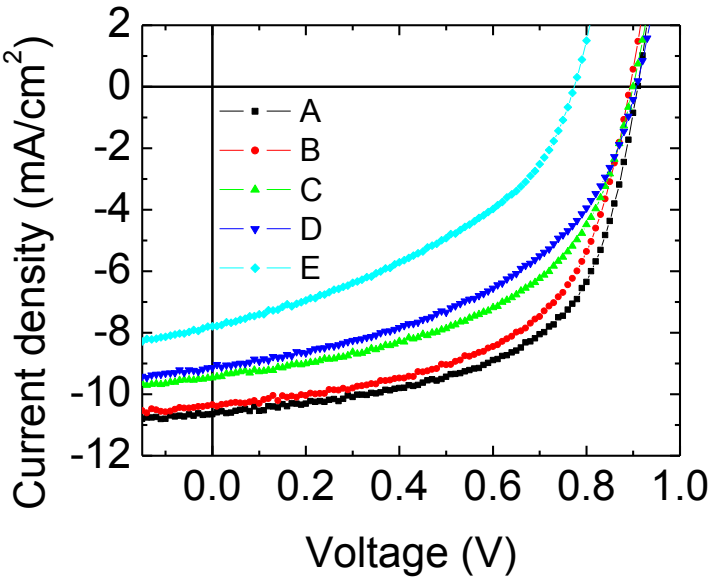

Figure 3. OPV cell performance of PCDTBT samples A to E with a structure of ITO/MoO_3/PCDTBT:$PC_{71}BM$/LiF/Al.

PCDTBT	J_{SC} (mA/cm^2)	V_{OC} (V)	FF (%)	PCE (%)
A	10.7	0.91	58.5	5.7
B	10.3	0.89	56.9	5.3
C	9.5	0.90	51.6	4.4
D	9.1	0.91	47.8	4.0
E	7.8	0.77	41.1	2.5

Table 2. Device characteristics of PCDTBT samples A to E.

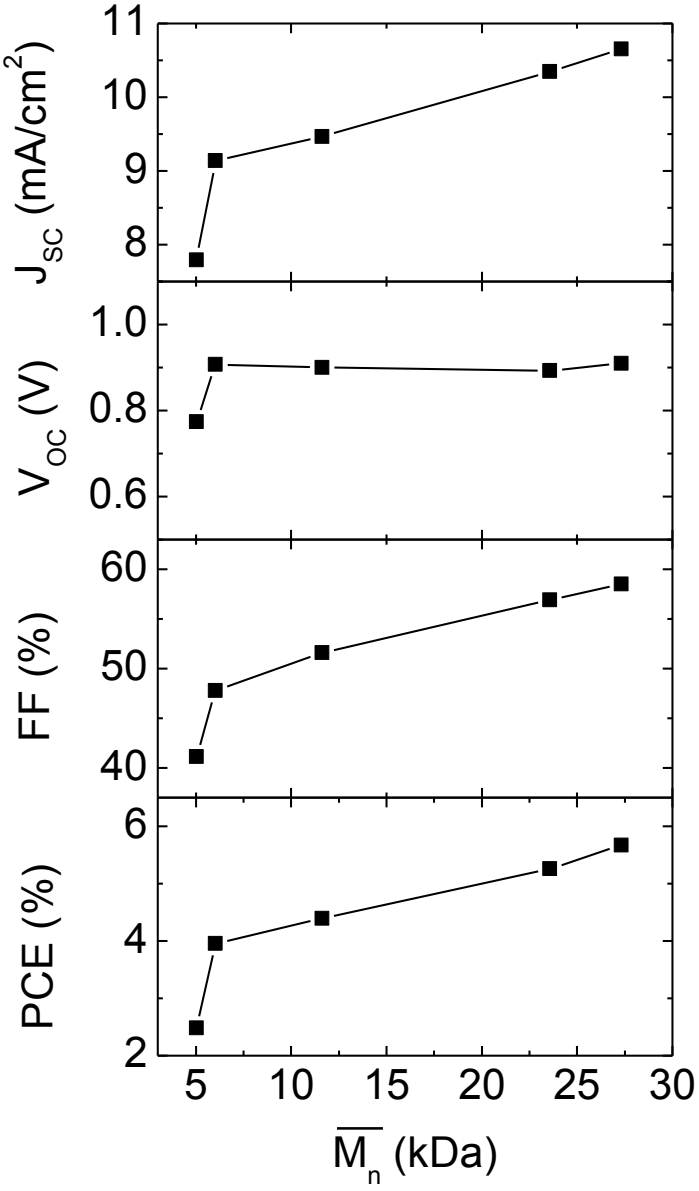

Figure 4. OPV cell parameters, J_{SC}, V_{OC}, FF, and, PCE vs the overall average molecular weight, $\overline{M_{\mathrm{n}}}$. J_{SC} and FF have strong correlations with $\overline{M_{\mathrm{n}}}$ resulting in higher PCE with higher $\overline{M_{\mathrm{n}}}$.

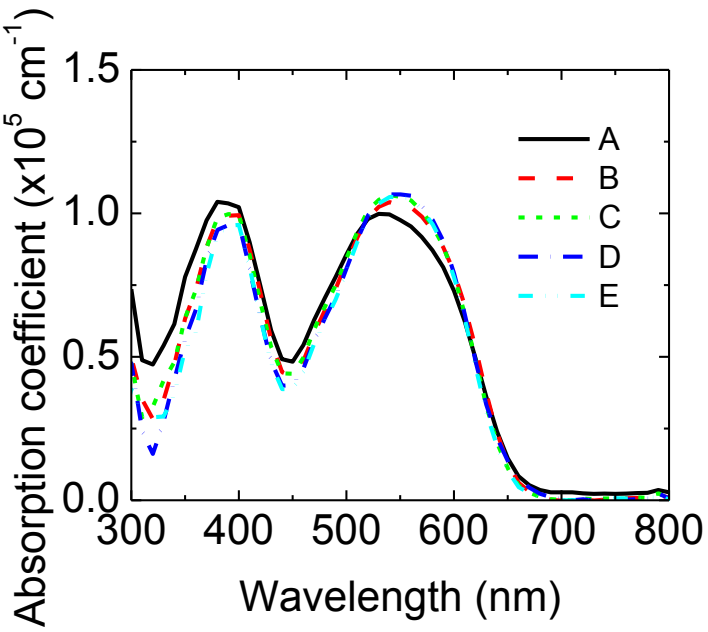

Figure 5. Absorption coefficients of PCDTBT A to E.

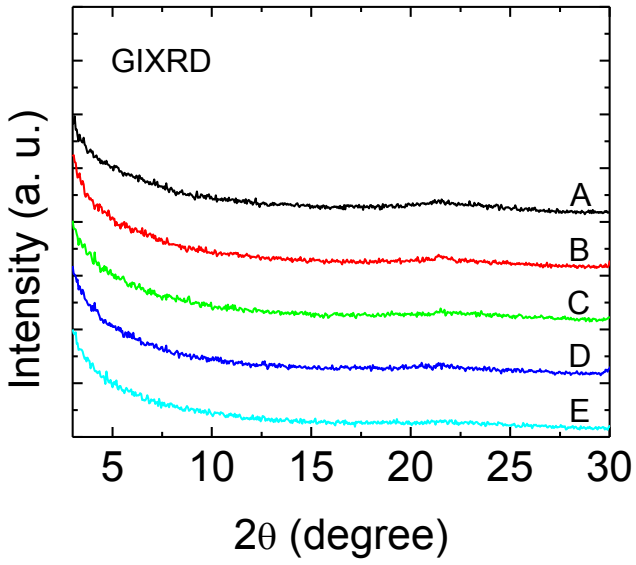

Figure 6. Grazing incident X-ray diffraction (GIXRD) data of PCDTBT samples A to E showing that PCDTBT A to E are essentially amorphous.

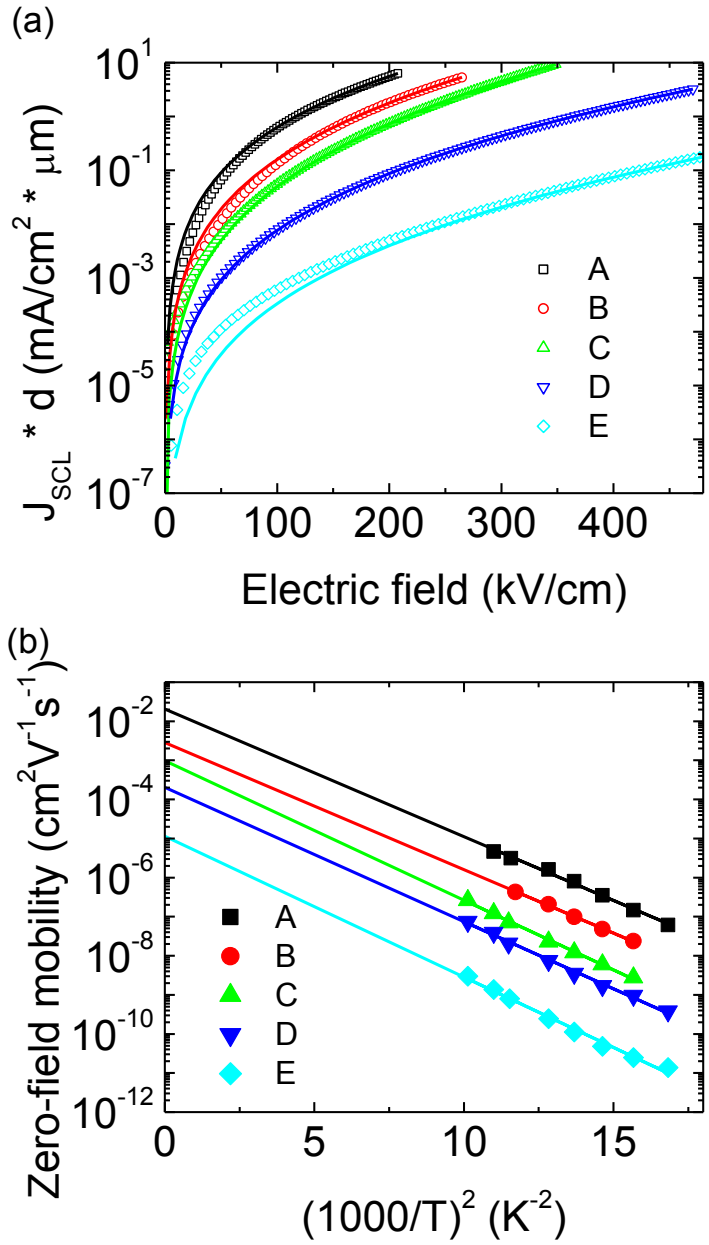

Figure 7. Transport data of PCDTBT A to E with hole-only configuration of ITO/MoO_3/PCDTBT/Au. a, *J-V* data and SCLC fittings (solid lines) at room temperature in semi-log plot (The log-log plot of the data and fitting are shown in Figure S1). b, Zero-field mobility against $1/T^2$ for GDM analysis. Similar slopes were observed indicating similar energetic disorder, σ, of the hole transporting sites of PCDTBT. The y-intercepts yield the high temperature limit mobilities, μ_∞.

PCDTBT	$\overline{M_n}$ (kDa)	μ_{Jsc} (cm^2/Vs)	μ_∞ (cm^2/Vs)	σ (meV)
A	27.3	2.7×10^{-5}	2.0×10^{-2}	112
B	23.6	7.4×10^{-6}	2.8×10^{-3}	112
C	11.6	2.5×10^{-6}	9.8×10^{-4}	117
D	6.0	3.6×10^{-7}	2.0×10^{-4}	115
E	5.0	1.6×10^{-8}	1.2×10^{-5}	118

Table 3. Transport parameters extracted from SCLC fitting and GDM analysis.

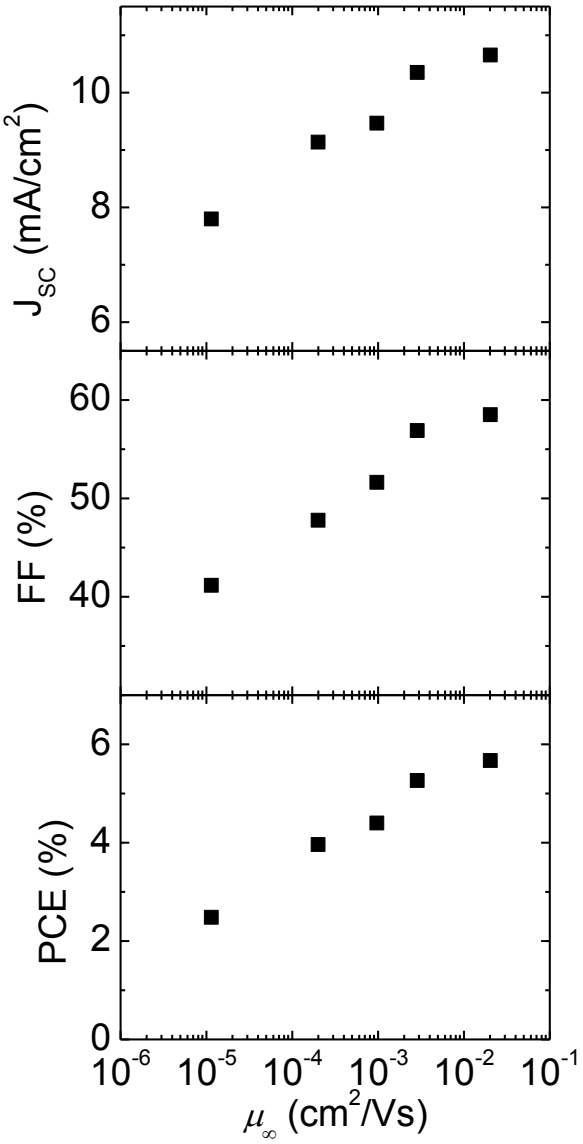

Figure 8. OPV cell parameters, J_{SC}, FF, and, PCE vs the high temperature limit mobility, μ_{∞}, of PCDTBT A to E.

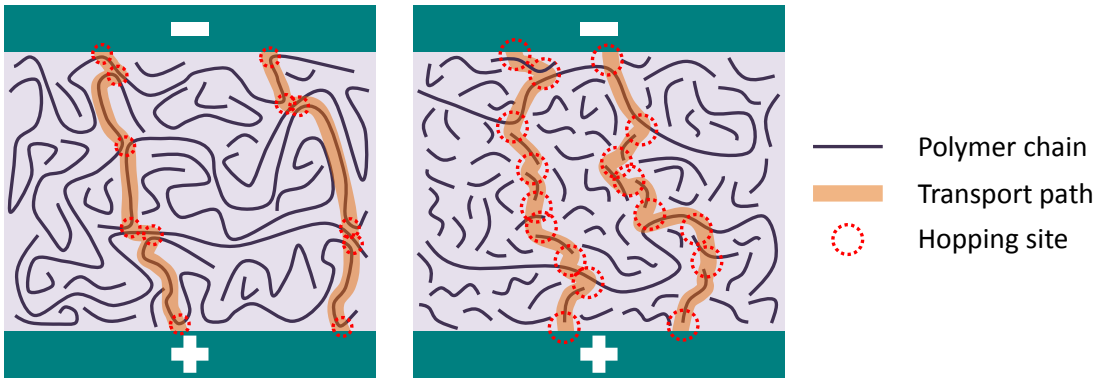

(a) High molecular weight (b) Low molecular weight

Figure 9. Schematic diagrams illustrating how charge carriers transport through a polymer layer. a, hole transport through a polymer layer with large fraction of high molecular weight polymer content. b, hole transport through a polymer layer with large fraction of low molecular weight polymer content.